Eur Biophys J (2012) 41:639–646
DOI 10.1007/s00249-012-0836-2

ORIGINAL PAPER

EBSA
Biophysics in Europe

Conformation and stability properties of B17: I. Analytical investigations using circular dichroism

Hassan M. Khachfe · David Atkinson

Received: 8 March 2012 / Revised: 24 April 2012 / Accepted: 25 June 2012 / Published online: 25 July 2012

Abstract Structural characterization of B17, the 17 % N-terminal domain of apo B, was carried out using circular dichroic (CD) spectroscopy, where secondary and tertiary structures were studied as a function of temperature and pH. Mild acidic conditions that correlate with histidine protonation invoked a change in the α-helix and random coil contents of the protein, with no apparent change in the β-sheet structural content. Specific changes in the structure of the protein that occur in response to temperature were also investigated to understand the stability and conformational changes of B17. Far- and near-UV CDs were used to probe the thermal changes in the protein. The protonation of some histidine residues was attributed to underlie the increase in the helical content of the protein.

Keywords Apolipoprotein B (Apo B) · Circular dichroism (CD) · Low-density lipoprotein (LDL)

H. M. Khachfe
Faculty of Sciences V, Lebanese University,
Nabatieh, Lebanon

H. M. Khachfe (✉)
Department of Biological and Biomedical Sciences,
Lebanese International University, P.O. Box 146404,
Mazraa, Beirut, Lebanon
e-mail: hassan.khachfe@liu.edu.lb

H. M. Khachfe · D. Atkinson
Department of Physiology and Biophysics,
and Center for Advanced Biomedical Research (CABR),
Boston University School of Medicine, 715 Albany Street,
Boston, MA 02118, USA

Introduction

Apolipoprotein B_{100} is the sole protein constituent of human low-density lipoprotein (LDL) and is one of the largest proteins known (Mahley and Angelin 1984). The primary sequence of the protein consists of 4,593 amino acids (aa), containing a 27-aa signal peptide. The molecular mass of the mature sequence is 512,937 Da, but when post-translationally glycosylated, the sugar moieties add some 30–40 kDa to the molecule, and the protein will have a molecular mass of ~550 kDa. (Chen et al. 1986; Cladaras et al. 1986; Knott et al. 1986; Law et al. 1986; Yang et al. 1986). While Apo B_{48}, the 48 % N-terminal portion of apo B_{100}, is made by intestinal cells via a novel splicing mechanism, the full-length protein is synthesized in the liver and packaged into VLDL within the inner leaflet of the endoplasmic reticulum (Olofsson et al. 1987; Pease et al. 1991).

Sixteen out of 25 cysteine residues in Apo B_{100} form disulfide bonds (Yang et al. 1990; Shelness and Thornburg 1996; Huang and Shelness 1997). Seven of these disulfide bridges occur in the 17 % N-terminal domain of the protein, all of which are found in regions that are released from the particle by trypsin digestion (Yang et al. 1989).

Due to the size and insolubility of Apo B_{100}, it is so difficult to determine the structural motifs responsible for the lipid association that only indirect probing has been done on this nonexchangeable protein. Biochemical, biophysical, and bioinformatical techniques have been used to study the domain structure and rearrangements of apo B (Nolte 1994; Khachfe 2002; Al-Ali and Khachfe 2007). Such approaches have explained much of the domain arrangement of this huge protein.

However, owing to its huge size and the lack of a crystal structure, it is imperative to study the structure of the

protein in pieces, probably corresponding to structural or functional domains. Accordingly, genetically engineered truncations have been obtained to study the domain organization in the protein (Cladaras et al. 1986; Herscovitz et al. 1991; Khachfe and Atkinson 2011). The 17 % N-terminal portion of the protein posed an interesting candidate for structural studies for several reasons: (1) its homology with lipovitellin—a lipid-transporting protein—whose structure was solved and opened the door to model the structure of apo B (Al-Ali and Khachfe 2007); (2) the optimal interaction of this portion of the protein is shown with the microsomal triglyceride transfer protein, MTP, which is an absolute requirement for the assembly of neutral lipids and phospholipids into chylomicrons and VLDL particles (Hussain et al. 1997); (3) this part of the protein readily associates with a variety of phospholipids to from large discoidal particles (Herscovitz et al. 2001) and has interesting metabolic behaviors based on its glycosylation state (Vukmirica et al. 2002); (4) as mentioned earlier, seven out of the eight disulfide bonds found in apo B_{100} are located in the N-terminal domain, suggesting that this portion is compact, highly organized, and most likely globular (Prassl and Laggner 2009).

Materials and methods

Pure B17 was obtained as previously described (khachfe and Atkinson 2011). Samples were dialyzed to the appropriate buffer conditions using Slide-A-Lyzer dialysis cassettes (10,000 MWCO) obtained from Pierce, USA.

Far- and near-UV CD spectra were measured and recorded on an Aviv 62DS CD Spectropolarimeter (Aviv Associates, Inc., Lakewood, NJ) equipped with a thermoelectric temperature controller. All spectra were recorded with a 0.5-nm wavelength scan step, 10.0-s average time, and 2.00-nm bandwidth.

The full scans were analyzed for their structural contents with the aid of CONTIN (Provencher and Glockner 1981) and PredictProtein (Bohm et al. 1992) computer packages. The analysis was done with the 35 matrix basis spectral set, which included the CD profiles of some 35 reference (all-α-helix, all-β-sheet, and α-helix and β-sheet) proteins.

Analysis of the CD thermal unfolding curves was carried out using the van't Hoff plots (Pace et al. 1989), ln K_{eq} versus $1/T$, where K_{eq} is the apparent equilibrium constant and T is the temperature in kelvin, as well as the first derivative plots of the temperature curves (Pace et al. 1989). If $\Theta_{obs}(T)$ is the observed ellipticity of the protein, $\Theta_F(T)$ and $\Theta_U(T)$ are the baselines for the protein folded and unfolded states determined by the temperature curves, then the equilibrium constant can be represented by

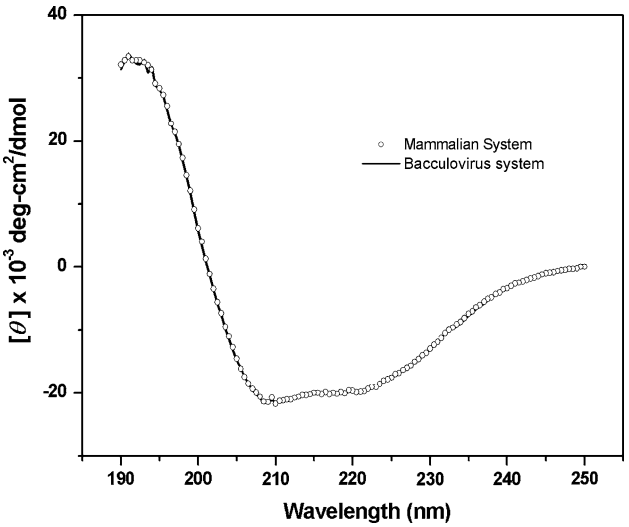

Fig. 1 Circular dichroism of B17. Far-UV CD spectra of B17 purified from mammalian and insect (bacculovirus expression, BV) cell systems. Mammalian B17 at 0.12 mg/ml in 5 mM K-phosphate, pH 7.4, at 25 °C, was compared to BV B17 at 0.12 mg/ml in 5 mM K-phosphate, pH 7.4, at 25 °C. Both measurements were carried out in a 2 mm-pathlength cell

$$K_{eq} = \frac{\Theta_F - \Theta_{obs}}{\Theta_{obs} - \Theta_U} \tag{1}$$

The plots were fitted—in the transition regions—by the linear function

$$\ln K_{eq} = \frac{\Delta S}{R} - \left(\frac{\Delta H_{vH}}{R}\right) \times \frac{1}{T}, \tag{2}$$

where $R = 1.98$ cal/mol K is the universal gas constant, and ΔS is the transition entropy.

Results

The full far-UV CD spectra of B17 from both expression systems are presented in Fig. 1. The data were recorded at 25 °C for 0.12 mg/ml B17 in 5 mM K-phosphate at pH 7.4. The CD data show that both mammalian and insect—bacculovirus expression (BV)—cell systems express the protein, as far as the secondary structure is concerned, with the same overall conformation. The spectrum is characterized by a broad negative curve between 208 and 225 nm as well as a positive peak at around 192 nm. This indicated that B17 is comprised of α-helix, β-strand (sheet), and turn and coil structures.

All subsequent pH, thermal behavior, and unfolding experiments using circular dichroic spectroscopy were done on B17 expressed and purified from both the mammalian and insect systems. Identical results were obtained irrespective of the protein source. Therefore, the results presented in this report show the data from the BV expressed protein only.

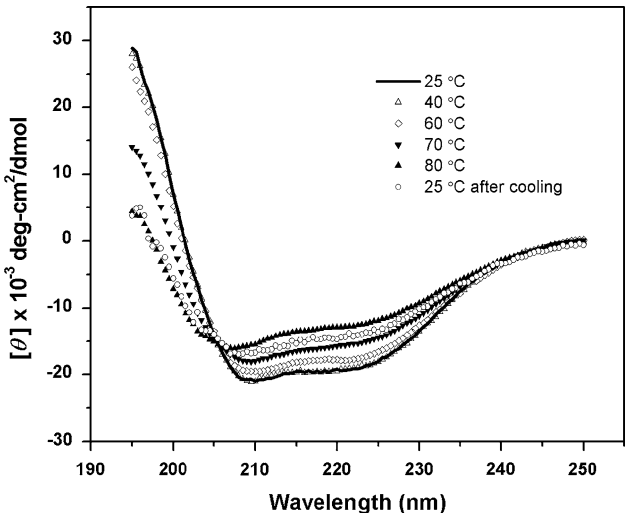

Fig. 2 Thermal behavior, I. Far-UV CD spectra of the baculovirus system (BV) B17 at 0.1 mg/ml in 5 mM K-phosphate, pH 7.4, recorded at constant temperatures of 25, 40, 60, 70, 80, and 25 °C after cooling, in a 2-mm-pathlength cell

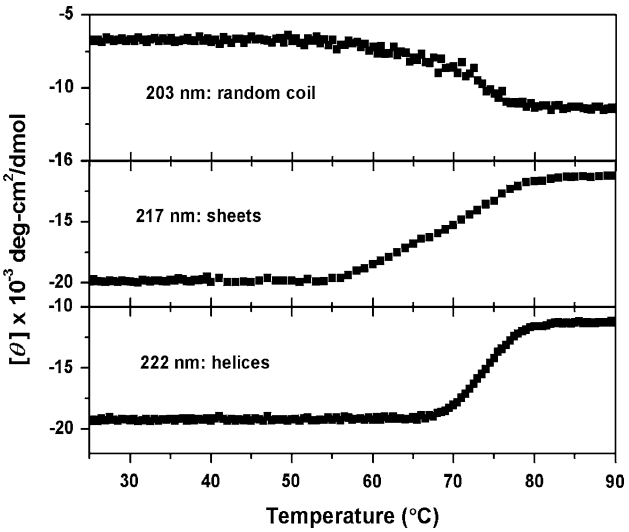

Fig. 3 Thermal unfolding of B17. Behavior of BV B17 as a function of temperature monitored at selected wavelengths: 203 nm (loops), 217 nm (β-sheet), and 222 nm (α-helix). The measurements were carried out on 0.1 mg/ml B17 in 5 mM K-phosphate, pH 7.4, in a 5-mm-pathlength cell

The concentration dependence of the CD of B17 was investigated by recording the CD of two samples in the same buffer at the same temperature: one at 0.1 mg/ml of B17; the other at 1 mg/ml of B17. Both spectra showed the exact same characteristics of the spectra in Fig. 1, and when normalized to concentration, the spectra were indistinguishable (data not shown). This relieved us from worrying about changes due to self-association in the range of concentrations we intended to use.

Figure 2 shows the full spectra of 0.12 mg/ml B17 from the baculovirus system (BV) in 5 mM K-phosphate at pH 7.4 recorded at constant temperatures of 25, 40, 60, 70, 80, and 25 °C after cooling. The spectra demonstrate the overall behavior of the protein at different temperatures and also provide its profile after it has been heated to elevated temperatures. The characteristic negative bands at ~208 and ~222 nm as well the positive bands at ~190 nm show—with varying degrees—the changes that are taking place to the different structural elements.

The specific thermal responses of the structural elements were monitored by thermally unfolding B17 at 0.12 mg/ml in 5 mM K-phosphate at pH 7.4 while recording the change in CD at 217 nm for β-sheets, 222 nm for α-helices, and 203 nm for loops. These measurements are shown in Fig. 3. The curves indicate that the α-helix, β-sheet, and turn and coil structures each undergo separate two-state, cooperative unfolding processes.

To examine the reversibility of the thermal unfolding in more detail, CD data were collected at these specific wavelengths, showing cooling at different rates. Figures 4 and 5 present the results of the cooling at different rates monitored at two wavelengths characteristic of the α-helix and β-sheet. The thermal unfolding of the β-sheets

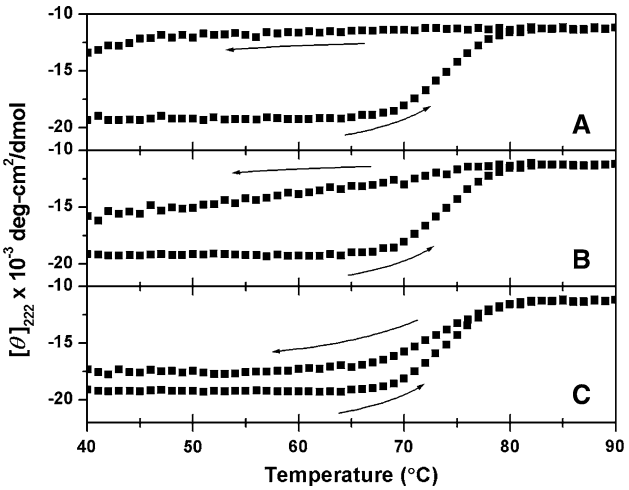

Fig. 4 Thermal behavior and reversibility of B17—I. The behavior (and its reversibility) of BV B17 as a function of temperature monitored at 222 nm (α-helix). Average time per point is: (*A*) 1 min, (*B*) 5 min, and (*C*) 10 min. The measurements were carried out on 0.1 mg/ml B17 in 5 mM K-phosphate, pH 7.4, in a 5-mm-pathlength cell

(monitored at 217 nm) up to ~70 °C—which is the approximate mid-temperature of the transition observed in Fig. 3 (217 nm)—refolded completely upon cooling, irrespective of the rate at which cooling took place. Subsequent unfolding and cooling at different rates produced results similar to those for the α-helix thermal unfolding. Visual inspection revealed that no aggregation was seen in any thermal unfolding experiment.

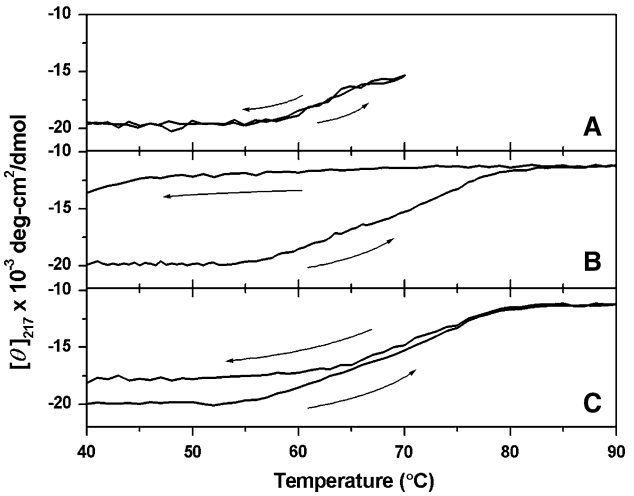

Fig. 5 Thermal behavior and its reversibility in B17—II. The behavior (and its reversibility) of BV B17 as a function of temperature monitored at 217 nm (β-sheet). Average time per point is: (*A*) 1 min, (*B*) 5 min, and (*C*) 10 min. The measurements were carried out on 0.1 mg/ml B17 in 5 mM K-phosphate, pH 7.4, in a 5-mm-pathlength cell

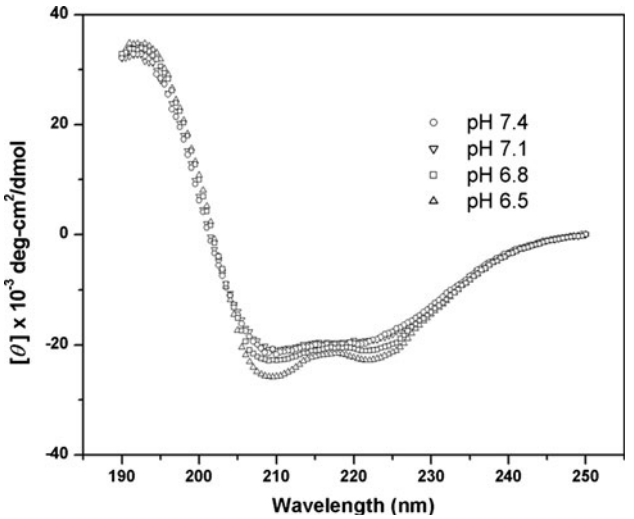

Fig. 6 pH behavior, I. The effect of pH changes on the structural elements of BV B17 at 0.1 mg/ml in 5 mM K-phosphate at selected pHs taken at 25 °C in a 2-mm-pathlength cell. The same sample was dialyzed to the desired pH, and its concentration was checked prior to recording the data

The behavior of B17 with respect to pH is shown in Fig. 6. The full spectra of 0.12 mg/ml B17 in 5 mM K-phosphate were recorded at a pH range from 7.4 to 6.5. Similar to the case of temperature change, the spectra corresponding to different pH points always retained characteristic negative and positive bands that correspond to the different structural elements in the protein. However, a progressive increase in the ellipticity was observed with decreasing pH, suggesting that conformational changes are taking place.

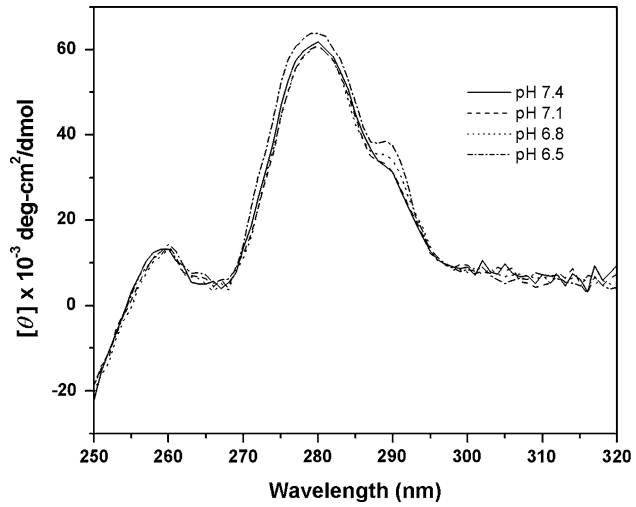

Fig. 7 pH behavior, II. Near UV-CD spectra of BV B17 at 0.5 mg/ml in 5 mM Na-phosphate, pH 7.4–6.5, and 25 °C in a 5-mm-pathlength cell. The same sample was dialyzed to the desired pH, and its concentration was checked prior to recording the data

The near-UV CD spectra of 1.5 mg/ml B17 in K-phosphate at 25 °C and pH 7.4, 7.1, 6.9, and 6.5, are shown in Fig. 7. The spectrum at pH 7.4 is characterized by a positive maximum at ~280 nm, with a shoulder at ~290 nm. These peaks have been reported to correspond to the tyrosine and tryptophan side chains (Kahn 1979; Strickland 1972, Strickland et al. 1972a, b; Strickland and Mercola 1976). Figure 8 shows the near-UV CD spectra of 1.5 mg/ml B17 in K-phosphate at 25, 40, 60, 70, and 80 °C. The basic spectrum characteristics are seen at 260, 280, and 290 nm.

Discussion

CONTIN and PredictProtein analysis of the far-UV CD spectrum of Fig. 1 shows that the secondary structure composition of B17 contains 29 % α-helix, 26 % β-sheet, and 45 % turns and random coil. A representative fit for such an analysis is shown in Fig. 9. These results are consistent with previously reported CD analysis of the protein (Herscovitz et al. 2001), as well as with the structure of the homologous region of lipovitellin (Mann et al. 1999). Table 1 gives a summary of the CD analysis of B17 and lipovitellin. The values in the "Measured CD" row, as well as the rest of the data in Tables 2 and 3, correspond to the deconvolution output ± SD of three to five average CD spectra for B17—recorded from three to five different samples under the same conditions of temperature and pH—with respect to a set of basis spectra.

Heating B17 caused the protein to undergo changes in all structural elements. Table 2 gives a summary of the deconvolution analysis of the spectra in Fig. 2. While these

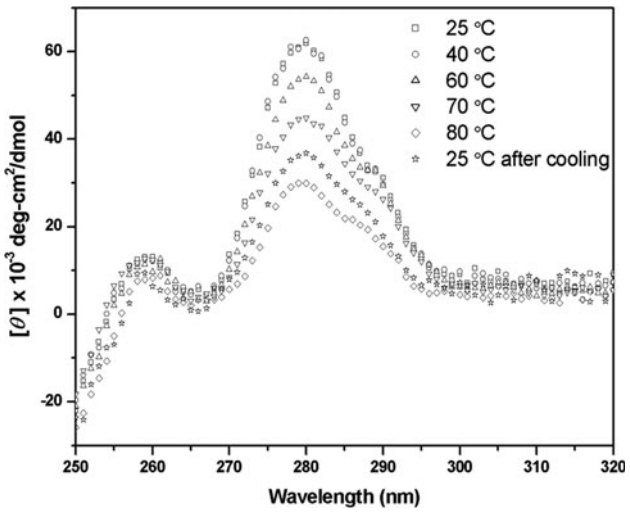

Fig. 8 Thermal behavior, II. Near-UV CD spectra of BV B17 at 0.5 mg/ml in 5 mM Na-phosphate, pH 7.4, recorded at constant temperatures of 25, 40, 60, 70, 80, and 25 °C after cooling, in a 5-mm-pathlength cell

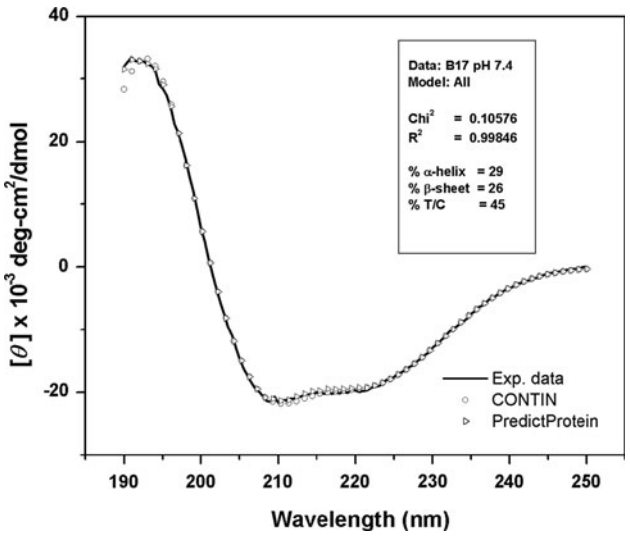

Fig. 9 CD analysis. A deconvolution analysis of the B17 CD spectrum of Fig. 1

spectra show that, upon heating the protein, all the structural elements are involved in the changes taking place, the table pinpoints the observation that these changes take place in phases. Between 25 and 40 °C, no recordable effect occurs. At around 60 °C, some of the β-sheet content begins to unfold to unordered turns and coils, so that by 70 °C, this change manifests itself clearly, whereas the unfolding of α-helices is just beginning. The unfolding of α-helices and β-sheets in this profile reaches its apex at around 80 °C when the content of both helix and sheet become around 10 %, whereas the percent content of turns and random coils is about 80 %. Upon cooling the protein back to 25 °C, the structural elements do not refold

Table 1 Far-UV CD analysis of B17 and lipovitellin

	% α-helix	% β-sheet	% Turns and coils
Measured CD	28.8 ± 0.6	25.6 ± 0.4	45.6 ± 0.8
Reported CD	30	27	43
Lipovitellin (B17 homology region only)	27	24	51

Percent occurrence of the different structural elements in B17 as measured in this study and reported by Herscovitz et al. (2001), and the comparison with the homology region of lipovitellin as determined by the count of residues per structural element reported in the crystal structure

Table 2 The change in the structural elements of B17 as a function of temperature

	% α-helix	% β-sheet	% Turns and coils
25 °C	28.8 ± 0.6	25.6 ± 0.4	45.6 ± 0.8
40 °C	29.1 ± 0.5	25.9 ± 0.1	46.0 ± 0.7
60 °C	28.9 ± 0.3	22.1 ± 0.4	49.0 ± 0.1
70 °C	25.2 ± 0.5	16.4 ± 0.6	58.4 ± 0.5
80 °C	12.4 ± 0.6	11.3 ± 0.2	76.3 ± 0.6
25 °C (after cooling)	15.1 ± 0.2	11.1 ± 0.6	73.8 ± 0.2

The table corresponds to the CD data reported in Fig. 2. Deconvolution analysis was carried out using CONTIN and PredictProtein. Standard deviations are calculated based on the values of repeated measurements under the same conditions

completely to their native state; rather, they adopt a conformation in which only some of the α-helices refold, while the β-sheets stay in their 80 °C unfolded state.

This thermal behavior is more apparent in the spectra of B17 as a function of temperature, as shown in Figs. 3, 4 and 5. These data show that the β-sheets begin unfolding at ~60 °C and continue to ~80 °C. The α-helices begin unfolding ~70 °C and after 10 °C reach an unfolded state plateau. Although the CD signal at 217 nm represents the sum of contributions of all structural elements, the fact that the helical content monitored—and solely contributed to by helices—at 222 nm does not begin to unfold until the 217 nm curve has passed its midpoint temperature is a clear indication that the 217-nm thermal unfolding curve is predominantly contributed to—at least up to ~70 °C—by the β-sheets of B17.

Figures 4 and 5 explore the reversibility of these thermal unfolding scans. In each figure, the curves show that while the unfolding process is similar at all three wavelengths, the refolding is kinetically controlled: the refolding of the α-helices is dependent on cooling and on time. In addition, Fig. 5 (upper panel) shows the complete reversibility of unfolding for the β-sheets should this unfolding stop at 70 °C. Beyond that, the sheets behave in a fashion similar

Table 3 The change in the structural elements of B17 as a function of pH

	% α-helix	% β-sheet	% Turns and coils
pH 7.4	28.8 ± 0.6	25.6 ± 0.4	45.6 ± 0.8
pH 7.1	28.2 ± 0.8	26.0 ± 0.3	45.3 ± 0.7
pH 6.8	30.4 ± 0.2	25.8 ± 0.5	43.8 ± 0.3
pH 6.5	32.3 ± 0.4	25.1 ± 0.7	42.6 ± 0.4

The table corresponds to the CD data reported in Fig. 6. Deconvolution analysis was carried out using CONTIN and PredictProtein. Standard deviations are calculated based on the values of repeated measurements under the same conditions

to the helices (lower panels). This may suggest that B17 is composed of two domains that, up to ~70 °C, are thermally independent, but beyond 70 °C, the two domains unfold—and eventually refold—cooperatively.

The rather unusually high melting temperatures for these structural elements in B17 compared to other apolipoproteins may be due to its special structural arrangement. For instance, disulfide bridges—six of which are found in B17—have been reported to cause a notable increase in the thermal stability of proteins (Wakarchuk et al. 1994). Engineered peptides as well as native proteins have shown that upon inclusion of a disulfide bridge, the thermal stability of an α-helix can increase by ~10 °C (Turunen et al. 2001; Wakarchuk et al. 1994).

The effect of pH change on the structure of B17 is summarized in Table 3. The data clearly show that upon decreasing the pH below 7.1, the α-helical content begins to increase, and the turn and coil structural content begin to decrease, with no substantial change in the β-sheet structure. At pH 6.5, the deviations from the pH 7.4 values for α-helix, β-sheet, and turns and coils become 3.5, −0.6, and −3 %, respectively. This shows that with a mild acidity change, the β-sheet content of B17 undergoes little or no change, while some residues that used to form turns and coils reorganize into α-helices. It is worth noting that below pH 6.5, the scans became irreproducible under the same conditions, suggesting further deterioration in the structure of the protein.

The near-UV CD spectra showed the behavior of the tyrosine and tryptophan residues as a function of temperature or pH. When correlated with the far-UV CD spectra taken at different temperatures, the thermal changes of the tyrosine and tryptophan residues can be associated with the individual unfolding of the β-sheets and α-helices, respectively. As the temperature was increased from 25 to 60 °C, only changes in the tyrosine CD (280 nm) were seen, concomitant with the change in β-sheet content seen in the full spectra. Beyond 60 °C, the changes are also associated with the thermal changes seen in the full spectra as well as the thermal unfolding scans of B17.

On the other hand, the fact that the change corresponding to pH in the tryptophan exposure is concomitant with the change in α-helical/coil content suggests that these residues are located in regions independent of the β-sheets. It might also suggest that there is some kind of domain arrangement in B17 in which the α-helices—or most of them—form a domain independent—at least with respect to pH—from the rest of the protein. A close look at the amino acid sequence of B17 reveals that the three tryptophans residues found in the protein are located in the second half of the structure. This gives the impression that the second portion of the sequence might comprise a good portion of an α-helical domain.

The reversibility upon prolonged cooling, observed when the heat capacity curve of a long-cooled sample looked almost identical to the heat capacity curve (Khachfe and Atkinson 2012), confirmed the CD observation concerning both the reversibility of the refolding and the kinetic nature of the process.

The CD data taken at characteristic wavelengths with respect to temperature attest to that. As was shown in Figs. 4 and 5, the CD measurements taken within a time frame similar to that of other calorimetry experiments (Khachfe and Atkinson 2012) did indeed show the irreversibility of the structure once it is heated beyond 70 °C. However, when the time step was increased to allow the protein more time before the acquisition of each data point, the CD measurement showed that B17 refolds almost to its original state.

Conclusions

Apolipoprotein B_{100} (apo B) is the only protein found on human low density lipoprotein (LDL) particles. LDL is the *agent provocateur* for atherosclerosis and other coronary heart diseases. Apo B is a large (4,536 amino acids, 550 kDa) secretory glycoprotein that has unique structural properties. The large size of apo B necessitated that it be studied in pieces corresponding to its structurally organized domains. In the present work, we studied the conformational and stability properties of the 17 % N-terminal domain of apo B, B17, based on its circular dichroic behavior. This portion of the protein is secreted predominantly lipid-free and plays an important role in the initiation and assembly of the LDL particle (Herscovitz et al. 2001).

Limited conformational and structural characterizations were carried out using far- and near-UV circular dichroic (CD) spectroscopy. The secondary structure and tertiary interactions were studied with CD as a function of temperature and pH. At 25 °C and pH 7.4, B17 is a globular protein comprised of 29 % α-helix, 26 % β-sheet, and

45 % turn and coil structures. The full far- and near-UV spectra of B17 at 25, 40, 60, 70, and 80 °C showed a gradual decrease in the α-helical and β-sheet structural content—with β-sheets unfolding first—concomitant with an increase in the structural content of turns and coils.

The full far-UV spectra at 25 °C showed an increase in the α-helical content upon decreasing the pH from 7.4 to 6.5, accompanied by an increase in the molar ellipticity of the near-UV CD peaks of tyrosine (280 nm) and tryptophan (290 nm).

Scanning the protein at specific wavelengths as a function of temperatures allowed for the determination of the melting temperatures of the different structural contents and the investigation of the reversibility of the unfolding upon cooling. These procedures revealed that the α-helices and β-sheets have melting temperatures of 73.5 and 69.9 °C, respectively. They also revealed that the refolding is kinetically controlled in that it depends both on temperature and time and that reversibility does indeed take place upon prolonged cooling.

The sequence of apo B_{100} has been proposed to adopt a pentapartite structure (Nolte 1994; White et al. 1994, Segrest et al. 2001), with the N-terminal region consisting of a globular domain that acts independently of the bulk lipid of the apo B-containing lipoprotein particle (Segrest et al. 2001). Truncation studies suggested an independent state of the amino-terminal region of the protein (Herscovitz et al. 1991).

Cryoelectron microscopic studies by Spin and Atkinson reported images of LDL at approximately 30 Å resolution. Some of these images were egg-shaped and contained a pointed end that was postulated to represent the N-terminal globular region ($\beta\alpha_1$) of apo B (Spin 1997). Poulos and Atkinson, as well as other researchers, also reported a knob-like electron-dense region on the surface of the LDL particle, with dimensions that approximate the βC globular domain of lipovitellin (Poulos 2001; Orlova et al. 1999).

Our circular dichroic results are consistent with these observations, as well as the previously reported CD results (Herscovitz et al. 2001), showing that the 17 % N-terminal region of apo B consists of a globular domain. In addition, the current work analyzed the thermal behavior of this $\beta\alpha_1$ domain independent of neighboring protein domains or lipid. It showed that while the full length apo B on either LDL particles or solubilized in NaDC has transition temperatures observed in other apolipoproteins (Walsh and Atkinson 1990), the independent B17 domain has considerably higher transition temperatures that may be the result of a tighter fold that it exhibits when it is not in contact with either other protein domains or a lipid core (Privalov 1982).

The behavior that B17 shows upon lowering the pH might be the beginning of a series of structural rearrangements that apo B_{100} undergoes following LDL endocytosis and the formation of the endosome. The endosome has an acidic milieu, which causes the LDL-receptor complex to dissociate so that the former begins the degradation process while the latter is recycled back to the cell membrane (Mathews and van Holde 1996). While we cannot at the moment relate between changes in the N-terminal region of apo B and the dissociation of the LDL receptor, it seems that changes to the overall structure of apo B begin to take place concomitant with the dissociation of the lipoprotein from the LDL receptor.

Acknowledgments Special thanks should go to Dr. D. Small and the late Dr. M. Walsh for their insightful discussions. This project was partially supported by an award from the National Institutes of Health (NIH).

References

Al-Ali H, Khachfe HM (2007) The N-terminal domain of apolipoprotein B-100: structural characterization by homology modeling. BMC Biochem 8:12

Bohm G, Muhr R, Jaenicke R (1992) Quantitative analysis of protein far UV circular dichroism spectra by neural networks. Protein Eng 5(3):191–195

Chen SH, Yang CY, Chen PF, Setzer D, Tanimura M, Li WH, Gotto AM, Chan L (1986) The complete cDNA and amino acid sequence of human apolipoprotein B-100. J Biol Chem 261(28): 12918–12921

Cladaras C, Hadzopoulou-Cladaras M, Nolte RT, Atkinson D, Zannis VI (1986) The complete sequence and structural analysis of human apolipoprotein B-100: relationship between apoB-100 and apoB-48 forms. EMBO J 3495–3506

Herscovitz H, Hadzopoulou-Cladaras M, Walsh MT, Cladaras C, Zannis VI, Small DM (1991) Expression, secretion, and lipid-binding characterization of the N-terminal 17 % of apolipoprotein B. Proc Natl Acad Sci USA. (Aug 15)

Herscovitz H, Derksen A, Walsh MT, McKnight CJ, Gantz DL, Hadzopoulou-Cladaras M, Zannis V, Curry C, Small DM (2001) The N-terminal 17 % of apoB binds tightly and irreversibly to emulsions modeling nascent very low density lipoproteins. J Lipid Res 42(1):51–59

Huang XF, Shelness GS (1997) Identification of cysteine pairs within the amino-terminal 5 % of apolipoproyein B essential for hepatic lipoprotein assembly and secretion. J Biol Chem 272(50):31872–31876

Hussain MM, Bakillah A, Jamil H (1997) Apolipoprotein B binding to microsomal triglyceride transfer protein decreases with increases in length and lipidation: implications in lipoprotein biosynthesis. Biochemistry 36(42):13060–13067

Kahn PC (1979) The interpretation of near-ultraviolet circular dichroism. Methods Enzymol 61:339–377

Khachfe HM (2002) Spectroscopic and calorimetric studies of the 17% N-terminal domain of apolipoprotein B-100. Ph.D. Dissertation, Department of Physiology and Biophysics, Boston University

Khachfe HM, Atkinson D (2011) Cloning, expression, purification, and quantification of the 17 % N-terminal domain of apolipoprotein b-100. J Cel Mol Biol (JCMB) 9(2):53–60

Khachfe HM, Atkinson D (2012) Conformation and stability properties of B17—II: analytical investigations using differential scanning calorimetry. Eur Biophys J (to be published)

Knott TJ, Pease RJ, Powell LM, Wallis SC, Rall SC Jr, Innerarity TL, Blackhart B, Taylor WH, Marcel Y, Milne R, Johnson D, Fuller M, Luisi AJ, McCarthy BJ, Mahley RW, Levy-Wilson B, Scott J (1986) Complete protein sequence and identification of structural domains of human apolipoprotein B 323:734–738

Law SW, Grant SM, Higuchi K, Hospattankar A, Lackner K, Lee N, Brewer Jr HB (1986) Human liver apolipoprotein B-100 cDNA: complete nucleic acid and derived amino acid sequence. Proc Natl Acad Sci USA 8142–8146

Mahley RW, Angelin B (1984) Type III hyperlipoproteinemia: recent insights into the genetic defect of familial dysbetalipoproteinemia. Advance in internal medicine. Year Book Med Publ Inc, Chicago, pp 385–411

Mann CJ, Anderson TA, Read J, Chester SA, Harrison GB, Kochl S, Ritchie PJ, Bradbury P, Hussain FS, Amey J, Vanloo B, Rosseneu M, Infante R, Hancock JM, Levitt DG, Banaszak LJ, Scott J, Shoulders CC (1999) The structure of vitellogenin provides a molecular model for the assembly and secretion of atherogenic lipoproteins. J Mol Biol 285(1):391–408

Mathews CK, van Holde KE (1996) Biochemistry. The Benjamin/Cummings, Menlo Park, CA, pp 623–630

Nolte RT (1994) Structural analysis of the human apolipoproteins: an integrated approach utilizing physical and computational methods. Ph.D. Dissertation, Department of Biophysics, Boston University

Olofsson SO, Bostrom K, Carlsson P, Boren J, Wettesten M, Bjursell G, Wiklund O, Bondjers G (1987) Structure and biosynthesis of apolipoprotein B. Am Heart J 113(2 Pt 2):446–452

Orlova EV, Sherman MB, Chiu W, Mowri H, Smith LC, Gotto AM Jr (1999) Three-dimensional structure of low density lipoproteins by electron cryomicroscopy. Proc Natl Acad Sci USA 96(15): 8420–8425

Pace CN, Shirley BA, Thomson JA (1989) Measuring the conformational stability of a protein. In: Creighton TE (ed) Protein structure, chap 13. IRL Press, New York, pp 311–330

Pease RJ, Harrison GB, Scott J (1991) Cotranslocational insertion of apolipoprotein B into the inner leaflet of the endoplasmic reticulum. Nature 353(6343):448–450

Poulos GW (2001) The three dimensional structure of low density lipoprotein via cryoelectron microscopy. Ph.D. Dissertation, Department of Biophysics, Boston University

Prass R, Laggner P (2009) Molecular structure of low density lipoprotein: current status and future challenges. Eur Biophys J 38:145–158

Privalov PL (1982) Stability of proteins. Proteins which do not present a single cooperative system. Adv Protein Chem 35:1–104

Provencher SW, Glockner J (1981) Estimation of globular protein secondary structure from circular dichroism. Biochemistry 20(1):33–37

Segrest JP, Jones MK, De Loof H, Dashti N (2001) Structure of apolipoprotein B-100 in low density lipoproteins. J Lipid Res 42(9):1346–1367

Shelness GS, Thornburg JT (1996) Role of intramolecular disulfide bond formation in the assembly and secretion of apolipoprotein B-100-containing lipoproteins. J Lipid Res 37:408–419

Spin JM (1997) Cryoelectron microscopy studies of low density lipoprotein in vitreous ice. Ph.D. Dissertation, Department of Biophysics, Boston University School of Medicine

Strickland EH (1972) Interactions contributing to the tyrosyl circular dichroism bands of ribonuclease S and A. Biochemistry 11(18):3465–3474

Strickland EH, Mercola D (1976) Near-ultraviolet tyrosyl circular dichroism of pig insulin monomers, dimers, and hexamers. Dipole-dipole coupling calculations in the monopole approximation. Biochemistry 15(17):3875–3884

Strickland EH, Billups C, Kay E (1972a) Effects of hydrogen bonding and solvents upon the tryptophanyl 1 L a absorption band. Studies using 2,3-dimethylindole. Biochemistry 11(19):3657–3662

Strickland EH, Wilchek M, Horwitz J, Billups C (1972b) Effects of hydrogen bonding and temperature upon the near ultraviolet circular dichroism and absorption spectra of tyrosine and O-methyl tyrosine derivatives. J Biol Chem 247(2):572–580

Turunen O, Etuaho K, Fenel F, Vehmaanpera J, Wu X, Rouvinen J, Leisola M (2001) A combination of weakly stabilizing mutations with a disulfide bridge in the alpha-helix region of *Trichoderma reesei* endo-1,4-beta-xylanase II increases the thermal stability through synergism. J Biotechnol 88(1):37–46

Vukmirica J, Nishimaki-Mogami T, Tran K, Shan J, McLeod RS, Yuan J, Yao Z (2002) The N-linked oligosaccharides at the amino terminus of human apoB are important for the assembly and secretion of VLDL. J. Lipid Res 43:1496–1507

Wakarchuk WW, Sung WL, Campbell RL, Cunningham A, Watson DC, Yaguchi M (1994) Thermostabilization of the *Bacillus circulans* xylanase by the introduction of disulfide bonds. Protein Eng 7(11):1379–1386

Walsh MT, Atkinson D (1990) Calorimetric and spectroscopic investigation of the unfolding of human apolipoprotein B 31:1051–1062

White JV, Stultz CM, Smith TF (1994) Protein classification by stochastic modeling and optimal filtering of amino-acid sequences. Math Biosci 119(1):35–75

Yang C-y, Yang T, Pownall HJ, Gotto AM Jr (1986) The primary structure of apolipoprotein A-I from rabbit high-density lipoprotein. Eur J Biochem 160:427–431

Yang C-y, Gu Z-W, Kim TW, Chen S-H, Pownall HJ, Sharp PM, Liu S-W, Li W-H, Gotto AM Jr, Chan L (1989) Structure of apolipoprotein B-100 of human low density lipoproteins. Arteriosclerosis 9:96–108

Yang C-y, Kim TW, Weng S-a, Lee B, Yang M, Gotto AM (1990) Isolation and characterization of sulfhydryl and disulfide peptides of human apolipoprotein B-100. Proc Natl Acad Sci 87:5523–5527